Bridging the gap between bio-inspired steering and locomotion: A Braitenberg Snake robot

I. Rañó[1] and A. Gómez Eguíluz[1] and F. Sanfilippo[2]

***Abstract*— Braitenberg vehicles are simple models of animal motion towards, or away from, a stimulus (light, sound, chemicals, etc). They have been widely used in robotics to implement target reaching and avoidance behaviours based on different types of sensors. While the seminal work of Braitenberg used wheeled vehicles to illustrate these principles of animal steering, few attempts have been made to combine these steering level controllers with other locomotion mechanism than active wheels. This paper presents the first implementation of a biologically inspired steering controller in a snake-like robot with passive wheels and active joints. The sinusoidal gait of the snake is modulated following the principles of the Braitenberg vehicles by using two sensors symmetrically located on the head. The effectiveness of this bio-inspired controller is shown through simulations where the snake orients its head and body with the direction of the stimulus gradient, and reaches the stimulus maximum within some range. This paper represents one of the first steps towards the connection of bio-inspired sensor based steering mechanisms and bio-inspired locomotion, and shows that existing theoretical results of Braitenberg vehicles with active wheels also apply to a snake-like robot with passive wheels.**

***Index Terms*— Bio-inspired robots, Braitenberg vehicles, snake-like robots.**

I. Introduction

Braitenberg vehicles are well known models biological steering implementing positive – and negative – taxis, i.e. the movement of an animal towards – or away from – a stimulus [1]. Because the seminal work of Valentino Braitenberg [2] focused on the principles connecting sensing to steering, his vehicles use wheels to abstract the locomotive systems of animals. This assumption has been experimentally found to match closely human trajectories at the steering level [3], i.e. trajectories are well described by the ones that the unicycle model dual-drive vehicles also follow. Although most of the current implementations of Braitenberg vehicles are based on wheeled robot the qualitative principles for the design of these steering level controllers can be extended to other types of locomotive mechanisms. This, in turn, opens the question of how to adapt the principles to locomotive systems other than active wheels, i.e. how to connect the steering and the locomotive systems for these bio-inspired steering controllers. This paper presents the first step toward bridging the existing gap in the connection between bio-inspired steering and locomotion. Using the principles of Braitenberg vehicles this work implements a positive taxis behaviour in a simulated snake robot with passive wheels (see figure 1), and shows that the resulting trajectories of the snake match the theoretical results obtained for wheeled vehicles with active wheels.

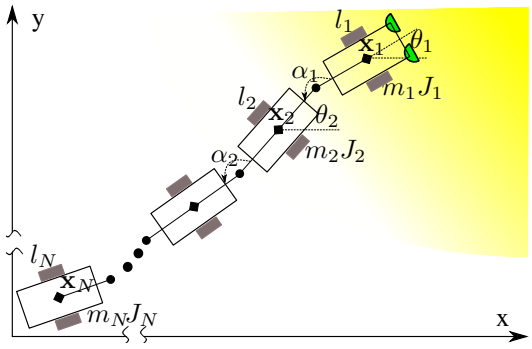

Fig. 1. Braitenberg snake robot with passive wheels

Simple animals with very different locomotive systems – flying, walking and crawling insects, for instance – can move towards a large variety of stimuli in the environment – sound, light, chemicals, etc – very effectively even in the presence of noise and disturbances. Likewise, there are many examples of wheeled robots moving successfully driven by different stimuli based on the principles of Braitenberg vehicles, yet most of these examples use active wheels as means of locomotion. Although it has been shown that simple (linear or non-linear) functions connecting sensors and actuators can generate the desired taxis movement [4], the principles are often used with dynamic connections that increase the dimension of the robots state. These principles were used to implement phonotaxis in wheeled vehicles using spiking neural networks in [5], where the sound perceived on the right and left "ear" was used to control the steering of a robot imitating female cricket phonotaxis. This work was later extended to outdoor robots that used whegs (active wheeled legs) to enable the robot to move in uneven terrains [6] [7]. The connections between the sensors and the motors generated positive taxis as a combination of vehicles 2a and 3b. Several models of auditory systems of animals have also been used in combination with Braitenberg vehicles to implement phonotaxis based on symmetrically placed microphones. A model of the central auditory system of a rat is used in [8] to implement sound source localisation based on the principles of vehicle 3a, while vehicle 2b was used in conjunction with a model of the auditory system of lizards in [9] [10]. The work in [11], a pioneering work in odour source localisation, presents an experimental

[1]I. Rañó and A. Gómez Eguíluz are with the School of Computing, Engineering, and Intelligent Systems, Ulster University. {i.rano,gomez_eguiluz-a}@ulster.ac.uk

[2]F. Sanfilippo is with the Department of Science and Industry Systems, Faculty of Technology, Natural Sciences and Maritime Sciences, University College of Southeast Norway (USN). filippo.sanfilippo@usn.no

analysis of vehicles 3a and 3b based on two chemical sensor located on both sides of a wheeled robot. Instead of using a dynamic connection, chemotaxis was implemented with a linear sensor-motor connection upon normalisation of the the sensor readings. A vehicle 2b for visual obstacle avoidance was presented in [12] using a dynamic connection between the two sides of an event camera image [13] and the robot's wheels. As we can see there are many instances of Braitenberg vehicles implemented usign non-proximity or 'unconventional' sensors, yet the work in [14] presents an implementation of vehicle 2b based on the readings of a laser scanner. This work proves theoretically and illustrates through experiments that the trajectories of this vehicle in a bounded environment can be chaotic, while the robot never hits any obstacle during its movement.

As stated above, most of the implementations of Braitenberg vehicles found in the literature are based on dual-drive robots with active wheels. Despite using active wheels, the work in [15] presents the implementation of robot phototaxis and obstacle avoidance using a passive steeting mechanism. A hardware implementation of a Braitenberg vehicle controls a motor that pulls from a string making a snake-like robot turn towards a light source. Although this is the first implementation of a Braitenberg vehicle for a snake robot it still uses active wheels, while the main novelty of the paper is the implementation of the passive steering mechanism. Braitenberg vehicles have been used to implement behaviours in non-wheeled robots, notably in fish robots. In [16] a robot endowed with pressure sensors symmetrically located on its head was shown to display rheotaxis behaviour – movement againts a water current – using the principles of Braitenberg vehicle 2b. The orientation performance of this bio-inspired controller was shown to be better, in terms of deviation with respect to the direction of a laminar flow, than other control mechanisms. It is worth noting that the movement of the fish head and body affects the measured pressure, but this seems no to have a negative effect on the rheotaxis performance. Another application to fish robotics is presented in [17], where an electric fish is steered using the differences between the currents sensed with electrodes located on the sides of the robot. The fish robot is attracted by conductive objects and avoids isolating ones inmersed in a whater pond. In the case of the electric fish, however, the steering is similar to wheeled vehicles as the fish is attached to, and controlled through, a rod, so the movement of the fish does not affect the sensor readings. One of the first attempts to integrate bio-inspired navigation and locomotion is presented in [18], where a quadruped robotic salamander is controller to perform phonotaxis in a simulated environment.

Through the literature we find multiple empirical applications of Braitenberg vehicles, although most rely on active wheels. This paper contributes to bring together bio-inspired steering and locomotion by implementing a Braitenberg vehicle 3a in a snake-like robot with active joints and passive wheels. The rest of the paper is organised as follows. Section II presents an overview of the derivation of the dynamic equations of the snake, the joint controller implemented, and the gait generation mechanism. This section also includes the modulation of the gait generation according to the principles of Braitenberg vehicles, specifically vehicle 3a. Simulations under a different set of stimulus functions are presented in section III, which shows how the proposed taxis approach works for our simulated locomotion mechanism. Finally, section IV ends the paper with some conclusions and future work directions.

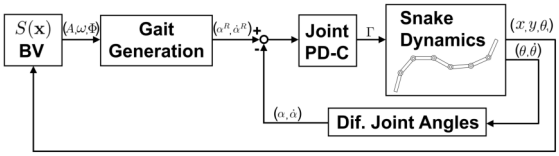

Fig. 2. The control architecture for the Braitenberg snake robot.

II. A Braitenberg vehicle model of a snake with passive wheels

This section presents the derivation of the model of the snake robot used and the control architecture represented in figure 2. Section II-A shows how the model of the simulated snake dynamics was obtained, and section II-B shows how the robot is controlled by a joint level PD controller (PD-C block) to track the movement gait signal. A sinusoidal pattern is outputted by the Gait Generator block, which sends the reference angular positions and velocities to the inner control loop, while the parameters of the gait generator are modulated through the implementation of a Braitenberg vehicle 3a using the sensors in the snake head. The outer controller, the Braitenberg vehicle (BV) block, receives as an input the pose of the head of the simulated snake, evaluates a stimulus function $S(\mathbf{x})$ at the points of where the sensors are located, and outputs the parameters for the gait generator.

A. Dynamic modelling of the snake robot

Let's assume an articulated robot with passive wheels and active joints like the one shown in figure 1. The robot has N links, $i = 1, \cdots, N$ and, therefore, $N-1$ actuated joints. Each link has mass m_i, inertia moment J_i, and length l_i. The wheels are located at the center of each link, which we assume corresponds to the centre of mass. Given the position of the first link $\mathbf{x}_1 = [x_1, y_1]$ and the orientations of all the links before the i-th (w.r.t. the inertial reference frame) θ_j $(j = 1, \cdots, i)$, we can compute the position of the centre of the link 'i' as:

$$\begin{aligned} x_i &= x_1 - \sum_{j=1}^{i} l'_j \cos\theta_j \\ y_i &= y_1 - \sum_{j=1}^{i} l'_j \sin\theta_j \end{aligned} \tag{1}$$

for $i > 1$, where $l'_j = \frac{l_j}{2}$ if $j = 1$ or $j = i$, and $l'_j = l_j$ otherwise. The kinetic energy for the link i is given by:

$$T_i = \frac{1}{2}\left[m_i(\dot{x}_i^2 + \dot{y}_i^2) + J_i\dot{\theta}_i^2\right] \tag{2}$$

where $\dot{x}_i$ and $\dot{y}_i$ can be obtained as the derivative of equation (1) w.r.t. time.

The wheels of the snake robot impose non-holonomic constraints on each link $\dot{x}_i \sin\theta_i - \dot{y}_i \cos\theta_i = 0$, and stating these constraints in terms of the Cartesian velocities of the head, the link orientations and angular velocities leads to:

$$\dot{x}_1 \sin\theta_i - \dot{y}_1 \cos\theta_i + \sum_{j=1}^{i} l'_j \dot{\theta}_j \cos(\theta_j - \theta_i) \quad = \quad 0 \quad (3)$$

for the i-th link ($i > 1$), while for $i = 1$ the constraint is $\dot{x}_1 \sin\theta_1 - \dot{y}_1 \cos\theta_1 = 0$. Defining the state vector $\mathbf{q} = [x_1, y_1, \theta_1, \cdots, \theta_N]$ equation (3) can be stated as a set of Pfaffian constraints $A(\mathbf{q})\dot{\mathbf{q}} = 0$.

Using Lagrangian mechanics and assuming the robot moves on a plane (i.e. $L = \sum_{i=1}^{N} T_i$) we can obtain the dynamic model of the robot:

$$M(\mathbf{q})\ddot{\mathbf{q}} + C(\mathbf{q}, \dot{\mathbf{q}})\dot{\mathbf{q}} \quad = \quad \Gamma - A(\mathbf{q})^T \lambda \qquad (4)$$

where $M(\mathbf{q})$ is the inertia matrix, $C(\mathbf{q}, \dot{\mathbf{q}})$ corresponds to the Coriolis and centrifugal forces, Γ is the set of generalised forces/torques, and λ is the vector of Lagrange multipliers that account for the constraint forces generated by the wheels. Using the derivative of the Pfaffian constraints with respect to time, $\dot{A}(\mathbf{q})\dot{\mathbf{q}} + A(\mathbf{q})\ddot{\mathbf{q}} = 0$, and equation (4) we can solve for λ and obtain the following equation for the restricted motion:

$$\begin{aligned} M(\mathbf{q})\ddot{\mathbf{q}} + C(\mathbf{q}, \dot{\mathbf{q}})\dot{\mathbf{q}} = \Gamma - A_M^{\dagger}(\mathbf{q})\dot{A}(\mathbf{q})\dot{\mathbf{q}} \\ + A_M^{\dagger}(\mathbf{q})A(\mathbf{q})M(\mathbf{q})^{-1}[C(\mathbf{q}, \dot{\mathbf{q}})\dot{\mathbf{q}} - \Gamma] \end{aligned} \qquad (5)$$

where $A_M^{\dagger}(\mathbf{q}) = A(\mathbf{q})^T \left[A(\mathbf{q})M(\mathbf{q})^{-1}A(\mathbf{q})^T\right]^{-1}$. Equation (5) allows simulating the dynamics of the snake robot with passive wheels and actuators in the joints. Next section will detail how equation (5) is used together with the joint level controller to generate the undulatory movement required for the snake robot to move forward.

B. Gait generation and independent joint position control

As first proposed by Hirose in [19], the forward motion of the snake is generated through a sinusoidal signal acting as a reference for each joint. The sinusoidal reference is characterized by a certain amplitude A and frequency ω and a specific phase shift between the joints. Because the reference undulation is applied to the angle between two consecutive links we can define the relative joint angle α_i as the difference of the angle of links $i + 1$ and i w.r.t. the inertial frame, i.e. $\alpha_i = \theta_{i+1} - \theta_i$. Specifically, the reference gait signals for the joints $i = 2, \cdots, N - 1$ are $\alpha_i^R(t) = A\sin[\omega t + \phi_i]$ where ϕ_i is the phase shift of the i-th joint relative to the neck (first joint) of the snake. The reference signal of the first joint is adapted to have an additional offset term Φ which allows the whole snake to steer, i.e. $\alpha_1^R(t) = \Phi + A\sin[\omega t]$. The forward velocity of the snake depends on the values of A and ω, while the offset angle Φ controls the direction of motion of the snake. These parameters can be tuned, together with the phase shifts between joints, to optimise the forward force pushing the snake robot forward, yet in this paper these values were selected empirically to have a good enough gait generator that allows to test the implementation of the Braitenberg vehicle. Finally, it is worth noting that the gait generation block also outputs the time derivatives of the joint reference signals $\dot{\alpha}_i^R(t)$ to be used by the inner joint controller.

The control of the joints is done through a PD controller for each independent joint, $\tau_i = K_p^i[\alpha_i^R(t) - \alpha_i(t)] + K_d^i[\dot{\alpha}_i^R(t) - \dot{\alpha}_i(t)]$, that tracks the corresponding reference position and velocity produced by the gait generator, where τ_i is the resulting torque applied to joint 'i', and K_p^i and K_d^i are the proportional and derivative gains of the controller. Although other control techniques [20] might lead to a more accurate tracking of the reference gait of the snake, the PD controller produced good enough results to implement the taxis behaviour in the snake. The controller gains were selected to be symmetric with respect to the centre of the snake, i.e $K_p^i = K_p^{N-1-i}$ and $K_d^i = K_d^{N-1-i}$. These joint torques (τ_i) are related to the generalised force/torques Γ in equation (5), and one can obtain the generalised torques from them. It is worth noting that because the robot has passive wheels the first two components of the Γ vector are zero, while $\Gamma_3 = \tau_1$, $\Gamma_4 = \tau_2 - \tau_1$, and so on until the last link. The values of the gains were adjusted using a constrained gradient descent on the least square position error $1/2 \sum_{t_k} \sum_{i=1}^{N-1} |\alpha_i^R(t_k) - \alpha_i(t_k)|^2$ for a reference trajectory of the joint angles $\alpha_i^R(t)$ during some simulation time $[0, t_f]$.

C. Braitenberg controller for the snake robot

In its simpler form Braitenberg vehicle 3a implements positive taxis towards a stimulus by setting the velocity of each wheel (left v_l and right v_r) to a decreasing function of the stimulus perceived on the same side sensor (located at $\mathbf{x}_l$, left, and $\mathbf{x}_r$, right). That means, for a stimulus function defined in the plane of movement of the robot, $S(\mathbf{x}) : \Re^2 \rightarrow \Re^+$, the velocity of the left/right wheels are computed as $v_{r/l} = F(S(\mathbf{x}_{r/l}))$, with $F(s) : \Re^+ \rightarrow \Re^+$ and derivative $F'(s) \leq 0$. From the analysis of the approximated motion equation of the wheeled robot with active wheels [4] it can be seen that the forward speed (v) control can be substituted by a controller, $v = F(\mathbf{x})$ using as sensor measurement the value of $S(\mathbf{x})$ at the point between the sensors $\mathbf{x} = \frac{\mathbf{x}_l + \mathbf{x}_r}{2}$. The turning rate ($\dot{\theta}$) control for the wheeled vehicle works similarly to a controller measuring at $\mathbf{x}$ the gradient of the stimulus in the direction perpendicular to the vehicle scaled by the derivative of $F(s)$, $F'(s)$. Therefore the control of the wheeled robot is based on a unique functional connection $F(s)$ which defines the forward velocity profile, while its derivative defines the robot turning rate.

In the case of the Braitenberg snake the control of the forward speed and turning rate is not so straightforward, as the motion direction is controlled by the offset angle in the neck joint (Φ), while the forward velocity depends on the amplitude and frequency of the sinusoidal gait generation function (A and ω). Therefore, we opted for implementing the controller based on the sensor readings of the left and right sensors using two different, but similar, functional

relations to modulate the gait parameters for turning direction and forward velocity. The angle offset for the neck was set to $\Phi(s_l, s_r) = \Phi_0 \tanh(\beta(s_r - s_l))$, where Φ_0 and β are parameter of the Braitenberg controller, and s_r and s_l are the instantaneous values read by the sensors of the snake robot, i.e. $s_r = S(\mathbf{x}_r)$ and $s_l = S(\mathbf{x}_l)$ on the right and left sensors of the head (see section III for the stimulus functions used). If the value of the stimulus function is the same on both sensors the offset will be zero and there will be no contribution of the Braitenberg controller to the steering signal Φ, i.e. the snake robot will oscillate along a straight line. If the measured value in the right sensor is larger than the value in the left sensor a positive offset is introduced in α_1 making the snake robot turn to the right, while it turns to the left in the opposite case. It is worth noting that we use the instantaneous readings of the sensors on the head, which is continuously oscillating, and therefore the generated offset will also oscillate resulting in the combination of two oscillatory signals with the same frequency.

The control of the forward velocity of the snake robot is based on the simultaneous modulation of the gait amplitude and frequency through the same modulating function $\eta(s_l, s_r)$, i.e. $A(s_l, s_r) = A_0 + A_1\eta(s_l, s_r)$ and $\omega(s_l, s_r) = \omega\eta(s_l, s_r)$. In this case the forward speed has to decrease as the stimulus value increases, which means the modulating function $\eta(s_l, s_r)$ needs to have a negative slope. Therefore, the selected function of the stimulus on the left and right sensors was chosen to be $\eta(s_l, s_r) = \frac{1}{2}\left[1 - \tanh(\gamma(\frac{s_r+s_l}{2} - s_0))\right]$ where s_0 and γ are parameters of the Braitenberg controller. While s_0 controls the range of stimulus values where the snake robot starts to slow down, and γ is a deceleration factor. It is worth noting that there is a fixed amplitude A_0 in the controller to avoid the snake to reach the singular configuration where all relative angles α_i are zero.

III. Experimental Results

This section presents result of the simulation of the Braitengerg 3a snake robot for several stimuli. In all the experiments performed the snake has 10 links with equal length ($l = 0.25$ m), identical mass ($m = 0.75$ kg) and inertia moment, and the distance between the sensors of the head was $\delta = 0.1$ m. A sinusoidal function with frequency $\omega = 0.9$ and amplitude $A = 0.5$ was used to generate the gait for the experiments where the forward speed of the Braitenberg controller is kept constant.

A. Braitenberg Snake in a constant gradient

It can be shown that the wheeled Braitenberg vehicle 3a performs a 'non-holonomic' descent in the stimulus function by aligning its orientation with the direction of the stimulus gradient [4]. Even in the presence of additive noise the average heading direction matches that of the gradient [21]. Since there is no theoretical result on whether a snake robot controlled using a Braitenberg vehicle will also perform such a descent in the stimulus function, this section will show through simulations that the robot indeed aligns its body with the direction of the gradient. Therefore, in this set of experiments the Braitenberg snake robot controller is evaluated for a linear stimulus $S(\mathbf{x})$ that increases along the x axis, i.e. $S(\mathbf{x}) = s_0 + \mathbf{m} \cdot \mathbf{x}$ were $\mathbf{m} = [b, 0]$. It is worth noting that the forward speed of the snake, i.e. the amplitude and frequency of the joint oscillations, is kept constant for this experiment, and only the heading offset Φ is applied.

Figure 3 shows the trajectories of the centre of mass of the proposed Braitenberg snake for 10 different initial configurations superposed with the plot of the stimulus, where bright colors represent a higher stimulus value. The position of the head of the snake is $x = 0$, $y = 0$, and the initial configuration of the snake was set randomly to have different orientations. Each trajectory was simulated until the corresponding snake reaches 30 m on the horizontal axis from the y axis. Although in some of the initial configurations the snake starts facing the direction opposite to the stimulus gradient, the robot always turns towards higher values of the stimulus and tends to align with the x axis. Since the component of the stimulus gradient $S(\mathbf{x})$ in the y direction is zero the y coordinate of the snake in the steady state depends on the random initial direction of the head. The figure shows that all the trajectories end up aligned with the direction of the stimulus direction, the x axis, for any initial orientation of the snake.

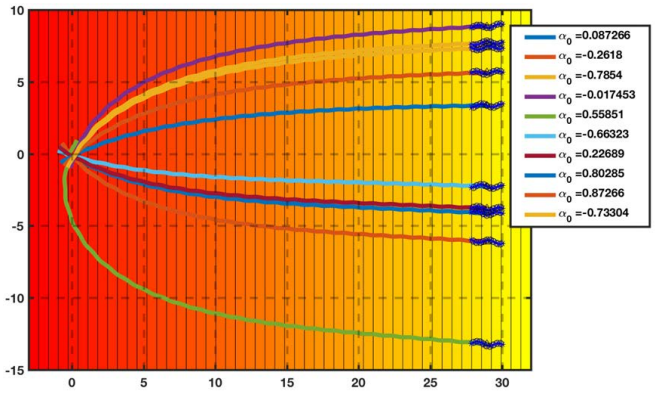

Fig. 3. Trajectories for 10 random initial orientations of the snake

1) Effects of the stimulus in the joints' oscillation: As mentioned above, the snake robot has to avoid the singular configuration where all α_i's are zero (the snake robot is fully stretched) or close to zero. This section investigates the effect of the steering control in the amplitude of the oscillation of the snake joints when the taxis controller is active. We performed simulations of the snake under two different conditions, constant stimulus and constant gradient stimulus for different gradient values. While the first case corresponds to a horizontal plane function, $S(\mathbf{x}) = s_0$, the latter corresponds to a non-horizontal plane, i.e. $S(\mathbf{x}) = s_0 + \mathbf{m} \cdot \mathbf{x}$ were we used $\mathbf{m} = [b, 0]$ for different values of b: 0.25, 1, 2.5, and 5.

Figure 4 shows the Fourier transform of $\alpha_i(t)$ resulting from the simulations for some joint angles of the snake in the range of frequencies of interest. As it can be seen

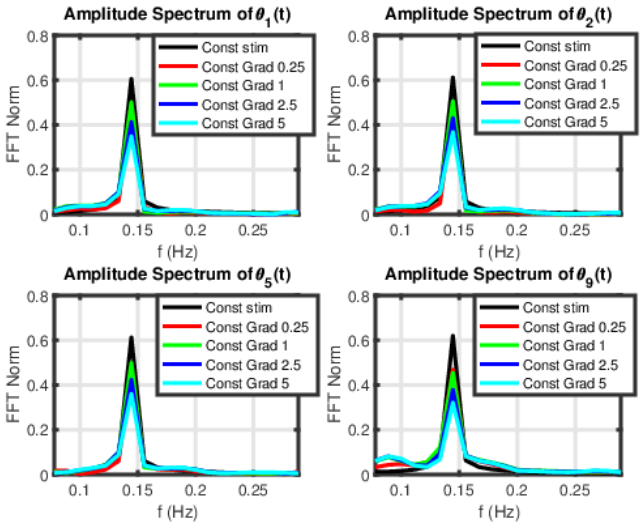

Fig. 4. Fourier transform of $\alpha_i(t)$

the amplitude of the oscillation decreases for all joints as the gradient increases, and for the case of zero gradient, i.e. constant stimulus, the oscillation amplitude is maximal. It could happen that the amplitude of the oscillation will be too small and the snake will be close to a singular configuration. Therefore, the parameters of the Braitenberg vehicle controller have to be carefully selected according to the range of gradients of the stimulus to avoid this situation.

B. Braitenberg Snake in a 2D linear-parabolic stimulus

As we just saw in the case of a linear stimulus function $S(\mathbf{x})$ there is a dispersion in the trajectories of the snake robot along the direction for which the gradient is zero. Using the same parameters of the Braitenberg controller for the offset of the head angle of the snake we changed the stimulus to add an inverted parabolic term to the stimulus in the y direction, i.e the stimulus function was set to $S(\mathbf{x}) = a_0 + bx + cy^2$ with $b > 0$ and $c < 0$ to make it linearly increasing in the horizontal direction while having a maximum at $y = 0$ for any value of x.

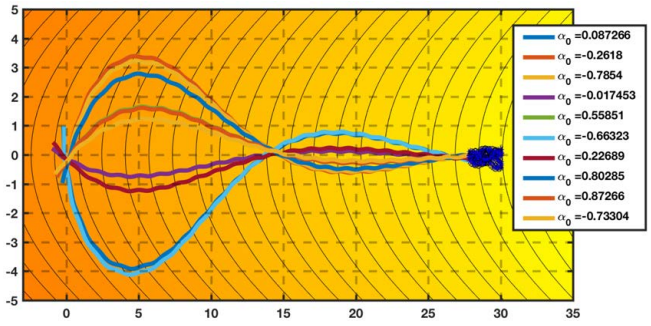

Fig. 5. Trajectories for 10 random initial orientations of the snake

Figure 5 shows the superposition of the stimulus $S(\mathbf{x})$ and the trajectories of the centre of mass of ten simulations of the Braitenberg snake robot in that stimulus. The initial position of the head for all simulations was $x = 0$ and $y = 0$ while the initial orientations were randomly generated, and the simulations were stopped once the head of the snake reached a distance of 30 m from the y axis. Like in the case of the linear stimulus the shake aligns its body with the x axis. However, because of the parabolic shape in the y direction with a maximum at $y = 0$, all the trajectories of the snake converge to the x axis, where the highest stimulus value is. It is worth noting that the trajectories of the snake oscillates around the x axis, a result which was previously obtained for wheeled Braitenberg vehicles 3a [22] from the analysis of the equations of motion under asymmetric stimulus functions.

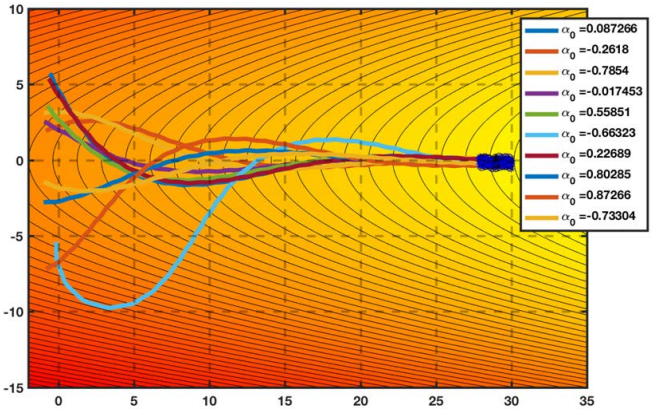

Fig. 6. Trajectories for 10 random initial orientations and y positions of the snake

Figure 6 shows the results of simulating ten trajectories with random heading directions and random initial positions of the head along the y axis. Like in the previous simulations the Braitenberg vehicle controller orients the snake robot in the direction of the increasing stimulus and aligns the body of the snake to the x axis. Oscillations with decreasing amplitude also occur here because of the asymmetry of the stimulus. The robot moves towards increasing values of x until the simulation is stopped (30 m) regardless of the initial y coordinate and orientation.

C. Snake control of heading and forward movement

This section presents the simulations of the Braitenberg snake robot in a parabolic stimulus function $S(\mathbf{x}) = g0 - \mathbf{x}^T D\mathbf{x}$ where g_0 is the maximum value of the stimulus and $D = dI_2$ is a scaled 2×2 identity matrix. The sign of the scale factor d has to be positive to ensure the stimulus has a maximum, while scaling the identity matrix represents an isotropic stimulus (the effect of an anisotropic stimulus was illustrated by the linear-parabolic case). While previous simulations kept the forward speed constant, i.e. constant amplitude A and frequency ω of the gait signal, this experiment illustrates the response of the robot when the forward speed is controlled through the shape function $\eta(s_r, s_l)$ introduced in section II-C.

Figure 7 shows the trajectories of the centre of mass of the snake robot in the parabolic stimulus for ten random initial

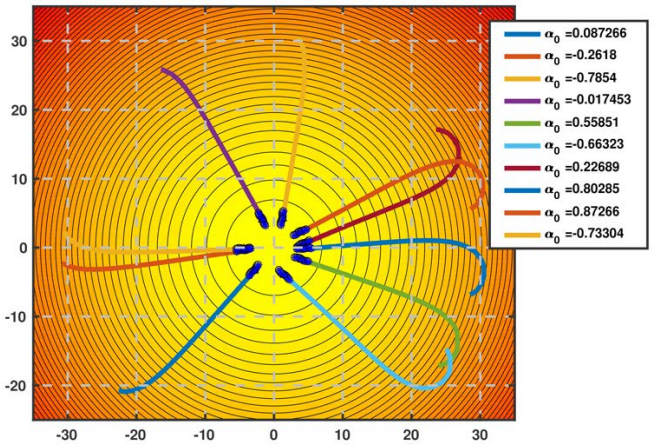

Fig. 7. Trajectories for 10 random initial positions and orientations of the snake

positions at 30 m distance from the origin, and with random orientations. The simulations show how the snake moves towards the stimulus maximum (located at the origin) while it reduces its velocity as the value of the stimulus increases, eventually stopping close to the maximum. It is worth noting that the closer the snake gets to the maximum the slower the oscillation frequency, hence the forward movement. Just like for wheeled Braitenberg vehicles the source is reached in infinite time.

IV. Conclusions and Further Work

This paper presents the implementation of a Braitenberg vehicle 3a in a snake-like robot. Although the seminal work on Braitenberg vehicles abstracts the locomotion mechanism of animals using wheels, this work showed that the biological principles underpinning the motion generation at the steering level can be applied to other locomotive systems. Interestingly theoretical results obtained for wheeled vehicles 3a also seem to apply to other locomotive systems, yet exact theoretical results for the undulatory movement of the snake are still an open question. Specifically, the simulations show that the body of the snake aligns with the direction of the gradient stimulus and the trajectory of the center of mass oscillates when the stimulus is asymmetric. The dimension of the system of differential equations describing the movement of the snake is much higher than for standard wheeled Braitenberg vehicles (3 dimensional) and it is still nonlinear, which makes the theoretical analysis much more complex.

Although experiments show are very positive results, the taxis controller drives the snake robot towards the maximum of the stimuli, one limitation of this work is the fact that the inner joint angle controller is not optimal, so a potential improvement will be to substitute the the inner loop PD controller by a better control mechanisms. Moreover, the generation of the gait signals in animals is done through Central Pattern Generators [23] instead of harmonic oscillators (i.e. sinusoidal signals) used in this work. In the future, the presented model may be useful for implementing path planning algorithms or obstacle-aided locomotion [24].

References

[1] G. S. Fraenkel and D. L. Gunn, *The orientation of animals. Kineses, taxes and compass reactions*. Dover publications, 1961.

[2] V. Braitenberg, *Vehicles. Experiments in synthetic psychology*. The MIT Press, 1984.

[3] G. Arechavaleta, J.-P. Laumond, H. Hicheur, and A. Berthoz, "An optimality principle governing human walking," *IEEE Transactions on Robotics*, vol. 24, no. 1, pp. 5–14, 2008.

[4] I. Rañó, "Biologically inspired navigation primitives," *Robot. and Auton. Sys.*, vol. 62, no. 10, pp. 1361–1370, 2014.

[5] B. Webb, *A Spiking Neuron Controller for Robot Phonotaxis*. The MIT/AAAI Press, 2001, pp. 3–20.

[6] A. Horchler, R. Reeve, B. Webb, and R. Quinn, "Robot phonotaxis in the wild: a biologically inspired approach to outdoor sound localization," *Advanced Robotics*, vol. 18, no. 8, pp. 801–816, 2004.

[7] R. Reeve, B. Webb, A. Horchlerb, G. Indiveri, and R. Quinn, "New technologies for testing a model of cricket phonotaxis on an outdoor robot," *Robot. and Auton. Sys.*, vol. 51, no. 1, pp. 41–54, 2005.

[8] M. Bernard, S. N'Guyen, P. Pirim, B. Gas, and J.-A. Meyer, "Phonotaxis behavior in the artificial rat psikharpax," in *Intl. Symposium on Robotics and Intelligent Sensors, IRIS2010*, 2010.

[9] D. Shaikh, J. Hallam, J. Christensen-Dalsgaard, and L. Zhang, "A Braitenberg lizard: Continuous phonotaxis with a lizard ear model," in *Proc. of the 3rd Intl. Work-Conf. on The Interplay Between Natural and Artificial Computation*, 2009, pp. 439–448.

[10] D. Shaikh, J. Hallam, and J. Christensen-Dalsgaard, "From "ear" to there: A review of biorobotic models of auditory processing in lizards," *Biological Cybernetics*, vol. 110, no. 4-5, pp. 303–317, 2016.

[11] A. J. Lilienthal and T. Duckett, "Experimental analysis of gas-sensitive Braitenberg vehicles," *Advan. Robot.*, vol. 18, no. 8, pp. 817–834, 2004.

[12] M. Milde, H. Blum, A. Dietmüller, D. Sumislawska, J. Conradt, G. Indiveri, and Y. Sandamirskaya, "Obstacle avoidance and target aquisition for robot navigation using a mixed signal analog/digital neuromorphic processing system," *Front. in Neurorobot.*, vol. 24, 2017.

[13] S. Liu and T. Delbruck, "Neuromorphics sensor system," *Current Opinion in Neurobiology*, vol. 20, pp. 288–295, 2010.

[14] I. Rañó, "The bio-inspired chaotic robot," in *Proc. of the IEEE Intl. Conf. on Robotics and Automation*, 2014, pp. 304–309.

[15] K. Ito and Y. Fukumori, "Autonomous control of a snake-like robot utilizin passive mechanism," in *Proceedings the IEEE International Conference on Robotics and Automation*, 2006, pp. 381–386.

[16] T. Salumäe, I. Rañó, O. Akanyeti, and M. Kruusmaa, "Against the flow: A braitenberg controller for a fish robot," in *Proc. of the Intl. Conf. on Robot. and Autom.*, 2012, pp. 4210–4215.

[17] V. Lebastard, F. Boyer, C. Chevallereau, and N. Servagent, "Underwater electro-naviagation in the dark," in *Proceedings of the International Conference on Robotics and Automation*, 2012, pp. 1155–1160.

[18] D. Shaikh, J. Hallam, J. Christensen-Dalsgaard, and A. J. Ijspeert, "Combining bio-inspired sensing with bio-inspired locomotion," in *The 5th International symposium on adaptive motion in animals and machines*, 2011, pp. 27–28.

[19] S. Hirose, P. Cave, and C. Goulden, *Biologically inspired robots: serpentile locomotors and manipulators*. Oxford University Press, 1993.

[20] E. Rezapour, K. Pettersen, P. Liljebäck, and J. Gravdahl, "Path following control of planar snake robots using virtual holonomic constraints," in *Proc. of the IEEE Intl. Conf. on Robotics and Biomimetics*, 2013.

[21] I. Rañó, M. Khamassi, and K. Wong-Lin, "A drift diffusion model of biological source seeking for mobile robots," in *Proc. of the IEEE Intl. Conf. on Robotics and Automation*, 2017.

[22] I. Rañó, "Results on the convergence of braitenberg vehicle 3a," *Artificial Life*, vol. 20, no. 2, pp. 223–235, 2014.

[23] A. Ijspeert, "Central pattern generators for locomotion control in animals and robots: A review," *Neural Networks*, vol. 21, no. 4, pp. 642–653, 2008.

[24] F. Sanfilippo, J. Azpiazu, G. Marafioti, A. A. Transeth, Ø. Stavdahl, and P. Liljebäck, "Perception-driven obstacle-aided locomotion for snake robots: the state of the art, challenges and possibilities," *Applied Sciences*, vol. 7, no. 4, p. 336, 2017.